Solvent-Probe NMR Imaging of Low-Density Polyethylene Rods: A Layered Structure Formed during the Molding Process

Masaharu OKAZAKI* and Kazumi TORIYAMA
Government Industrial Research Institute, Nagoya, Hirate, Kita-ku, Nagoya 462
(Received April 12, 1993)

The spatial inhomogenuity of a linear low-density polyethylene rod shaped with a metallic mold was clearly imaged by the solvent-probe NMR imaging technique. Images with T_2 contrast were obtained using the T_2-flash sequence, which reflects the spatially resolved mobility of the solvent molecules absorbed in the polymer. The NMR image was very much dependent on the thermal history both during and after the molding process. These results were interpreted with the aid of the nuclear relaxation parameters of the matrix polyethylene determined by the high-resolution solid state NMR technique. It is suggested that the solvent-probe NMR imaging technique provides valuable information concerning the micro structure (domain structure) and its spatial distribution of a crystalline polymer.

Although the NMR imaging technique has been applied to medicine with great success, its application to material science is rather limited.[1] This may be mainly because direct imaging of a rigid sample is difficult to apply, and has been achieved mainly by NMR specialists with modest success.[2] Among solid materials, elastomeric materials can be imaged rather easily and some interesting information has been obtained.[3,4] Although the short T_2 of a proton prevents any observations of the NMR image of a rigid solid material, this short T_2 allows one to observe absorbed solvents or gases selectively without any disturbance from the matrix signal.[5] Koenig et al. observed the image of a PMMA rod partially swollen with methanol, and found that the type of solvent-diffusion into the polymer is the so-called case II.[6] Hui et al. carried out the same kind of study, and analyzed the solvent diffusion process with a theoretical model.[7] These successful studies suggest that the difficulty to observe images of rigid materials is not a shortcoming of the method, but an advantage for studying many phenomena in solid materials, including transport phenomena and chemical reactions.

In a previous study,[8] we obtained an NMR image of a polyethylene rod by observing the NMR signal of cyclohexane absorbed in the polymer. The swelling process was quasi-equilibrated after a long treatment (8 h at 323 K) of the shaped rod with cyclohexane. We chose cyclohexane as the solvent probe for the following reasons: (1) it gives a single proton signal, (2) it penetrates into polyethylene at a moderate temperature (323 K) without dissolving the polyethylene. In the present study a clear spatial inhomogenuity was observed for a polyethylene rod shaped with a mold; the spin–spin relaxation time of the solvent molecules (T_2(P)) were determined at different positions in the rod from several images observed after different T_2(P) decay periods. In addition, the cause of this spatial inhomogenuity, observed as an "solvent-probe NMR image", was analyzed through the observation of high-resolution solid state ^{13}C NMR for different regions of the polyethylene sample.

Experimental

Linear low-density polyethylene (LLDPE; d=0.92, butene content = 7.0 wt%, MW = 1.1×10^6) was a gift from Mitsubishi Petroleum Company Limited. High-density polyethylene was purchased from Aldrich Chemicals. Molten (softened) polyethylene was shaped into a rod (3.0 ϕ, 40 mm long or 4.0 ϕ, 30 mm long; ϕ represents diameter) or plate (1×10×40 mm) using a mini-molder (Custom Scientific Instrument, CS-183 MMX) at 460 K after kneading for more than 10 min under an N_2 atmosphere. After squeezing the polyethylene melted at 460 K into a mold cooled at ca. 273 K (stainless steel; 12×25×45 mm 103 g for 3.0 ϕ, or 12×25×35; 80 g for 4.0 ϕ), it was immediately cooled with water at ca. 273 K for obtaining a "rapidly quenched (abbreviated hereafter as RQ-) sample". For preparing "gradually cooled (abbreviated as GC-) polyethylene rods", the mold was heated to about 353 K before squeezing the softened polyethylene into the mold. The mold containing polyethylene was left standing until it was cooled spontaneously (for about 10 min). Samples were soaked into cyclohexane in an NMR tube (4.1 ϕ) to allow the solvent to penetrate into the sample for a period of 11 h at 323 K; they were then subjected to observation without removing the solvent. γ-Ray irradiation was carried out in the air at a does rate of about 30 kGy h^{-1} for 20 h.

NMR-imaging observations were performed at R.T. using the spin-warp[9] 2D-FT method with a Bruker MSL-200 NMR spectrometer equipped with an NMR-microscope attachment. Phase-encoded 128 gradient (or spin) echos were accumulated at a repetition time of 3.0 s. A T_2 contrast was made by applying 90°(X)—180°(Y)—90°(−X) pulses before the imaging pulses. A sinc pulse (3-robes) of about 45 degree was employed as a selective excitation pulse in order to obtain a sliced image of the sample rod at a thickness of about 1.0 mm. The details are shown as sequence 1 in Fig. 1. During the repetition time, proton magnetization of the solvent molecule absorbed in the polyethylene rod recovered to its thermal equilibrium value, since T_1, determined by spin echo images observed with a series of repetition times, was 0.55 s. The high-resolution solid state ^{13}C NMR spectra, the proton spin lattice relaxation times measured indirectly both in the laboratory frame (T_1(H)) and in the rotating frame ($T_{1\rho}$(H)), and the ^{13}C spin lattice relaxation time

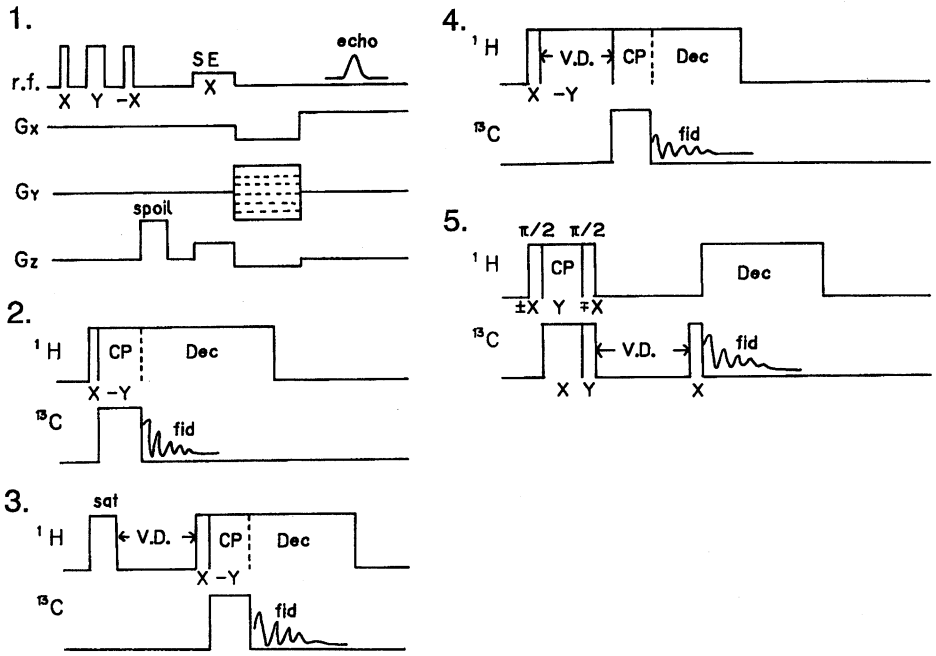

Fig. 1. Pulse sequences used in the present study. In the diagrams, SE, Dec, and CP represent the pulses for selective excitation, proton decoupling, and cross polarization, respectively. V.D. represents the variable delay for relaxation measurements. ±X, ±Y indicate the phases of the rf-pulses. (1) T_2 flash imaging: G_x, G_y, and G_z represent gradient field pulses for frequency encoding, phase encoding, and slice selection, respectively. The first three pulses: $X(\pi/2)$, $Y(\pi)$, and $-X(\pi/2)$ are applied to prepare the spin–spin relaxation effect on the static magnetization. The spoiling pulse destroys the transverse magnetization. (2) CP with high power proton decoupling: this pulse sequence is usually used to obtain "CP-MAS" spectrum by spinning the sample cell at the magic angle from the magnetic field direction. Pulse sequences (3) and (4) are used to measure proton T_1 and $T_{1\rho}$ (represented as T_1(H) and $T_{1\rho}$(H)), respectively, by transferring the proton magnetization to ^{13}C nucleus by CP sequence and thus observing the ^{13}C signal. (5) Torchia's sequence[10] to observe ^{13}C spin lattice relaxation.

(T_1(C)), were obtained using the respective pulse sequences of 3—5 (Fig. 1) with the same NMR spectrometer. The relaxation parameters, except for T_1(H), were determined by a nonlinear least-squares fitting of the observed relaxation curves with assuming two ($T_{1\rho}$(H)) or three (T_1(C)) exponential decays.[11] The density of polyethylene was estimated by floating the sample piece in a mixture of cyclohexanol and iso-propyl alcohol.

Results

Although the density of the polyethylene (LLDPE) indicated by the maker is 0.920, it changed slightly depending on the molding procedure: the densities for the outer and inner regions of the RQ-sample (3.0 ϕ) were slightly less than the announced value (0.916 and 0.919, respectively); those for the GC-sample, however, were slightly larger (0.925 and 0.925, respectively) than this value. The weight gain during the cyclohexane treatment was also basic data in the present study. Those during a treatment for 11 h were 12.4% of the original weight for both the RQ- and the GC-samples (3.0 ϕ); they increased slightly up to 16.7 and 18.3%, respectively, after an additional treatment for 22 h (33 h in total). An observation of the NMR images was made after a treatment for 11 h. Although the sample rod may slightly swell, the microstructure must be preserved, since a sample rod recovered the original diameter and appearance after drying.

Figure 2 shows solvent-probe NMR images at several T_2 decays for a rapidly quenched LLDPE rod (3.0 mm ϕ, length=40 mm), showing a section in a plane perpendicular to the long axis (symmetry axis) of the rod. The intervals between the two 90-degree pulses (see, pulse program 1 in Fig. 1) for photographs 1—6 are 0, 2.0, 4.0, 8.0, 14.0, and 20.0 ms, respectively. The outermost white ring is the image of neat cyclohexane with which the polyethylene rods were treated. The inner part is a sectional image of the polyethylene rod, which was observed indirectly by using the signal of cyclohexane molecules absorbed in it. Although the appearance of the sectional surface had no inhomogenuity, a layered structure was clearly observed in the solvent-probe NMR image for RQ-polyethylene rods. The image of a sample rod shaped and cooled gradually (as described in the Experimental section) was almost homogeneous. The former image of the polyethylene rod comprises three regions: (1) the outer region, which becomes dark from the third photograph (region 1), (2) the intermediate region (region 2), and (3) the innermost region (region 3), which persists even in the last

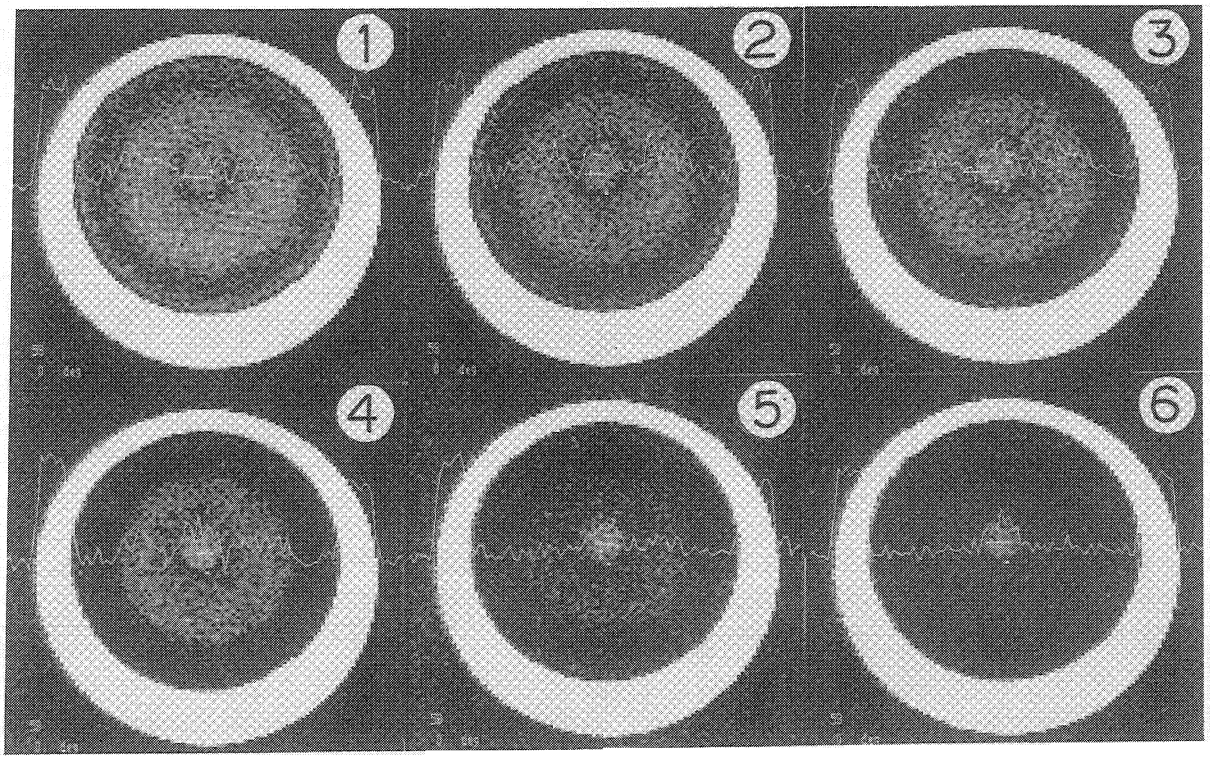

Fig. 2. Solvent-probe NMR image of a rod (3.0 ϕ, 40 mm long) shaped from molten LLDPE with a metallic mold. The polyethylene is rapidly quenched by a cooled mold made of stainless steel (100 g). The intervals between the two 90 pulses (X and $-X$ in pulse program 1 in Fig. 1) for photographs 1—6 are: 0, 2.0, 4.0, 8.0, 14.0, and 20.0 ms, respectively.

photograph. Although the first two regions appear reproducibly on both samples with diameters of 3.0 and 4.0 mm, unless the sample was gradually cooled, the innermost region appears only in the RQ-sample with a diameter of 3.0 mm. A similar structure was also observed for high-density polyethylene rods. Although the image for the GC-sample was almost homogeneous, the inner portion, corresponding to region 2 for the RQ-sample, was chosen as a representative for comparing with other systems.

Figure 3 shows semi-logarithmic plots of the image levels (which are proportional to the NMR signal for each position) for the two regions (region 1 and 2) of the 3.0 ϕ sample against the time for spin–spin relaxation, including the time from the selective excitation pulse to the echo. The slopes therefore correspond to T_2(P)'s, the proton spin–spin relaxation time of the probe molecules absorbed in the two corresponding regions. T_2(P) for region 1 was 3.8 ms, whereas that for region 2 was 17.8 ms. This means that the solvent molecule in region 1 is considerably immobilized, compared with that in the interior (region 2). Although we did not make a plot for region 3, the core, it is obvious that T_2(P) in this region is of the order of 100 ms or more. As can be seen in Fig. 3, when the plot is extrapolated to zero time, the intercepts for the two regions are almost the same. Therefore, the concentration of the absorbed solvent is almost homogeneous throughout the sample. We should correct our previous erroneous conclusion that the difference in the concentration of the solvent in the two regions is the cause of the layered structure in the solvent-probe NMR image.[8)]

Figure 4 shows semi-logarithmic plots of the image levels against the time of T_2 decay for region 2 of the GC-(a) and RQ-LLDPE rods (b) with a diameter of 4.0 mm. The slopes correspond to 9.6 ms and 14.0 ms for the GC- and the RQ-samples, respectively. This indicates that the motional freedom of the probe molecule is considerably larger in the inner part of the RQ-sample, compared with that in the GC-sample. It is also noteworthy that T_2(P) for region 2 of the RQ-sample of 3.0 ϕ is considerably longer than that of the corresponding value for the 4.0 ϕ sample.

To investigate the relation between the solvent-probe NMR image and the solid state character of the matrix polyethylene, the high-resolution solid-state ^{13}C NMR spectra of the matrix were observed. Figure 5 shows the CP-MAS NMR spectra of LLDPE rods shaped by either rapid quenching or slow cooling in the mold. Spectra **a** and **b** are of the outermost region (region 1) and the inner part (region 2), respectively, of the RQ-sample (4.0 ϕ), and spectrum **c** is of the inner part of the slowly cooled one. A contact time of 1.0 ms was employed, since the magnetization increases to the maximum level

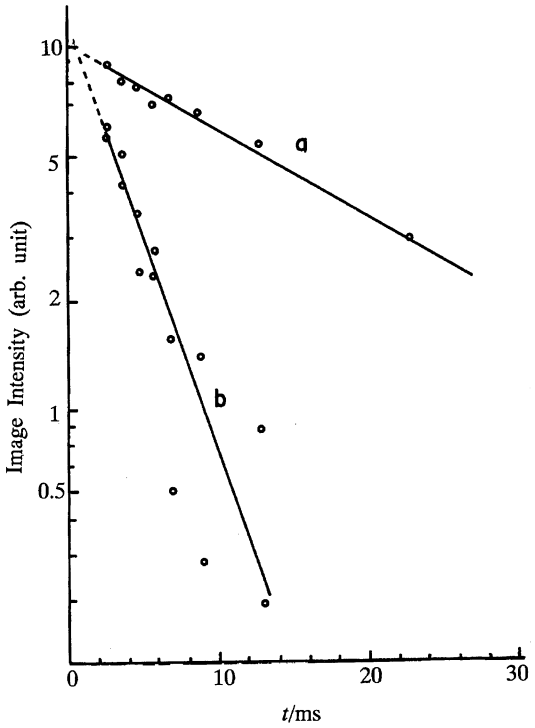

Fig. 3. Semilogarithmic plots of the image intensity of the two regions: **a**, the outer layer and **b**, the inner layer of the RQ-sample.

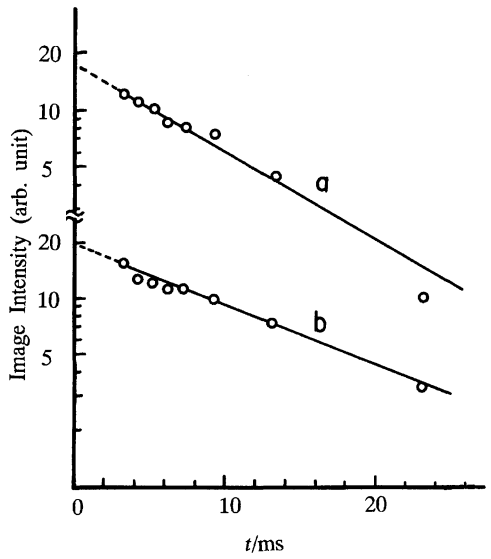

Fig. 4. Semi-logarithmic plots of the image intensity for the inner region of polyethylene rods (4.0 ϕ and 30 mm long) shaped by a stainless-steel mold (80 g). **a**: rapidly quenched, **b**: slowly cooled.

within this CP time. The signal decreases with a further increase in the contact time due to the fact that $T_{1\rho}$(H) is rather short and is on the order of 4—10 ms. The shoulder at a few ppm upfield from the main peak has been assigned to the amorphous carbon.[12] By reconstructing the spectra with two Lorentzian lines, the

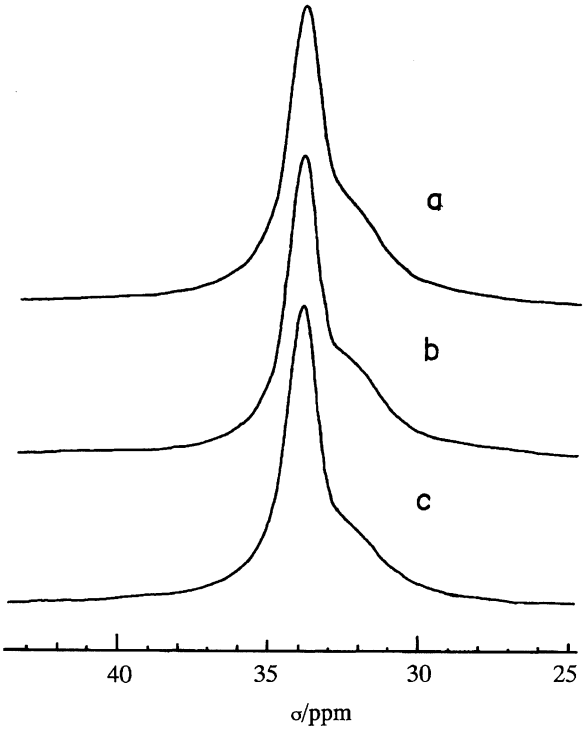

Fig. 5. ^{13}C CP-MAS NMR spectra of linear low-density polyethylene shaped with a metallic mold. **a** and **b** are the spectra for the outer and the inner regions, respectively, of the RQ-sample, and **c**: the inner region of the GC-sample. The diameter of the sample rod was 4.0 mm.

percentages of the amorphous region were estimated to be 33, 30, and 28% for regions 1 and 2 of the RQ-, and the inner region (corresponds to region 2) of the GC-samples, respectively. Thus, the difference in the content of the amorphous region is very small when a comparison is made between regions 1 and 2 of the RQ-sample or between region 2 of the RQ- and GC-samples.

T_1(H) and $T_{1\rho}$(H) were determined on the three systems mentioned above by nonlinear least-squares fittings of the relaxation curves observed with pulse sequences 3 and 4 (in Fig. 1), respectively; the results are listed in Table 1. The relaxation curves for $T_{1\rho}$(H) at the main peak (originated mainly from the trans–trans conformation of the molecular chain) for the three systems are shown in Fig. 6. T_1(H) and $T_{1\rho}$(H) for the amorphous part were obtained by plotting the signal intensity at 2.0 ppm upfield from the main peak. Although the relaxation curve for T_1(H) is fitted well by assuming single exponential decay kinetics, that for $T_{1\rho}$(H) requires two exponential decay functions for a satisfactory reproduction. T_1(C)'s which were determined by nonlinear least-squares fitting (with three exponential functions) of the signal heights at the main peak, are given in Table 2. The percentage below each T_1(C) and $T_{1\rho}$(H) values are the relative contribution of the components associated with those T_1(C) and $T_{1\rho}$(H) to the total signal intensity. Although the

Table 1. ^{1}H Spin Relaxation Parameters of Polyethylene Samples[a)]

	Crystalline				Amorphous			
	T_{1H}	$T_{1\rho}$(H;1)	$T_{1\rho}$(H;2)	$T_{1\rho}$(H;av)	T_{1H}	$T_{1\rho}$(H;1)	$T_{1\rho}$(H;2)	$T_{1\rho}$(H;av)
Rapid(outer)	0.6s	10.2 ms	2.3 ms(36%)	6.5 ms	0.6s	9.6 ms	3.1 ms(69%)	4.5 ms
Rapid(inner)	0.52s	14.0 ms	2.5 ms(24%)	10.1 ms	0.52s	8.9 ms	2.5 ms(47%)	5.1 ms
Grad (inner)	0.58s	11.8 ms	2.0 ms(27%)	8.2 ms	0.58s	16.2 ms	2.7 ms(79%)	3.9 ms

a) T_{1H} represents spin lattice relaxation time in the laboratory frame, and $T_{1\rho}$(H;1), $T_{1\rho}$(H;2), and $T_{1\rho}$(H;av) are those in the frame rotating at the resonance frequency. $T_{1\rho}$(H;1) the longer value and $T_{1\rho}$(H;2) the shorter one were obtained from the non-linear least square fitting of the relaxation curve by assuming two exponential functions, while $T_{1\rho}$(H;av) is that obtained by assuming single exponential relaxation function. The fraction of the shorter $T_{1\rho}$-component is given in the parenthesis.
The sample rods were shaped in either rapid quenching or gradual cooling conditions, as indicated Rapid or Grad on each row. The portion which was cut out for the measurement is indicated by "outer" or "inner" for the outer and the inner regions, respectively, of the sample rod, whose diameter is 4.0 mm. "Crystalline" and "Amorphous" at the top row indicates that the parameters below which were determined at the crystalline peak at about 34 ppm and at the shoulder at about 32 ppm due to the amorphous part, respectively.

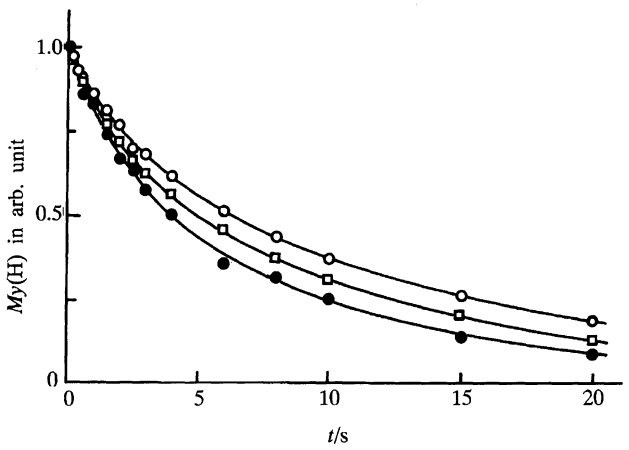

Fig. 6. Plots for $T_{1\rho}$(H) of the inner region (region 2) of the RQ-polyethylene rod (upper;○), the same part of the GC-rod (middle;□), and the outer region (region 1) of the RQ-rod (lower;●). The solid lines represent the results of least square fitting using two exponential curves whose parameters are listed in Table 1.

Table 2. ^{13}C Spin Lattice Relaxation Parameters of Polyethylene Samples[a)]

	T_1(C;1)	T_1(C;2)	T_1(C;3)
Rapid(outer)	97.9 s	6.5 s	0.42 s
	49.6%	25.7%	24.7%
Rapid(inner)	152.2 s	6.9 s	0.40 s
	55.1%	27.1%	17.8%
Grad (inner)	196.7 s	15.9 s	0.49 s
	48.3%	25.4%	26.3%

a) T_1's are obtained by the non-linear least square fitting of the relaxation curves by assuming three exponential functions. The percentage represents the ratio of the component associated with each relaxation parameter. The observed systems are: the outer region ("outer"; first row) and the inner part ("inner"; second row) of the RQ-sample rod, and the inner part of the GC-sample rod. Diameter of the rod was 4.0 mm.

shortest T_1(C) value is assigned to the amorphous part, the percentage below the T_1(C) value does not mean the percentage of the amorphous part in the polymer. The ratio of the amorphous part should be considerably larger than this value, since the peak position for the gauche conformation, the main component contributing to the amorphous region, is about 2 ppm apart from the main peak; only its shoulder contributes to the signal height at the main peak position.

It is known that the thicker is the lamellar thickness, the longer are $T_{1\rho}$(H) and T_1(C) of the crystalline portion.[13)] As can be seen in Fig. 6, spin-lattice relaxation in the rotating frame for region 1 of the RQ-sample, region 2 of the GC-sample, and region 2 of the RQ-sample proceed at speeds of this order. The ^{13}C-spin relaxation for region 1 of the RQ-sample was considerably faster than the other two systems, which show relaxation curves that are similar to each other, though the individual parameters are different. Therefore, region 1 of the RQ-sample has a considerably smaller lamellar thickness, compared with the inner parts of both the gradually cooled and rapidly cooled ones. It is also interesting to note that $T_{1\rho}$(H) for region 2 of the RQ-sample is longer than that for the GC-sample, i.e. the crystallite of the former is thicker than that of the latter.

Discussion

1. Physical Properties of the Outer Layer of a Rapidly Quenched Sample. The intercepts of the relaxation plots in Figs. 3 and 4 indicate that the solvent is absorbed at an approximately equal density in the two regions of the RQ-rod as well as in the GC-rod; the image contrast is thus made entirely by T_2(P) (T_2 of the probe molecule), which is a measure of the mobility of the probe molecule. Since the solvent molecules in the outer layer (region 1) of the RQ-sample have a short T_2(P), they are immobilized due to close contact with the polymer matrix, probably because the space for the accommodation of the solvent molecule is finely divided.

As can be derived from the relaxation parameters given in Tables 1 and 2, region 1 of the RQ-sample rod is

characterized by both shorter T_1(C) and $T_{1\rho}$(H) for the crystalline region. Since these parameters are related to the thickness of the lamellar,[13] that in region 1 of the RQ-sample is considerably smaller compared with that of other systems. In the same way, since $T_{1\rho}$(H) for region 2 of the RQ-sample monitored at the main ^{13}C resonance is considerably longer than that for the GC-sample, the lamellar thickness for the former is longer than the latter. The densities of these systems, ^{13}C CP-MAS NMR spectra (Fig. 5), and the ^{13}C relaxation experiment (Table 2) suggest that there is only a small difference in the amorphous/crystalline ratio between these systems. Therefore, the thickness (or dimension) of the amorphous region also becomes smaller in the same order for the lamellar thickness: i.e. region 2 of RQ-sample>GC-sample>region1 of RQ-sample.

A very small difference between the $T_{1\rho}$(H;av)'s monitored at the crystalline peak (6.5 ms) and at the amorphous shoulder (4.5 ms) is an additional evidence for this small domain structure in the outermost region of the RQ-sample. A small difference in the relaxation parameters for the two domains indicates that: (1) the two $T_{1\rho}$'s are partially averaged by the proton spin exchange over the two domains, or (2) the two domains have solid state characteristics similar to each other. Since the CP-MAS NMR spectrum of trace a in Fig. 5 is clearly divided into two parts, the first case is more plausible. The rapid spin exchange over the two domains indicates that the dimension of the domain structure is small. The $T_{1\rho}$(H;av)'s for the two domains of the other systems are much different from one another, as given in Table 1, indicating larger domain structure.

This interpretation was reinforced by the observation that when a sample was irradiated by gamma-rays at a does of 0.6 MGy, T_2(P) of the absorbed cyclohexane decreased from 14.0 ms to 8.2 ms for the GC-sample (4.0 ϕ) and from 9.6 ms to 6.6 ms for region 2 of the RQ-sample. Since most of the free radicals decay upon a cyclohexane treatment, the decrease in T_2(P) (T_2 of probe) is solely due to the fact that the solvent molecule absorbed in the irradiated polyethylene is immobilized to a greater extent. This immobilization of the probe molecule can be explained by the decrease in the compartment room for the probe molecules (or micro-droplet of the solvent) due to radiation-induced cross linking between the polymer molecules.

2. Layered Structure of the Molded Polyethylene. As shown in Fig. 2, the NMR image for the innermost part of the sample rod appears to be bright, even after the T_2-decay for more than 20 ms. This occurs only for the RQ-sample, and can be explained using a model in which the solidification of the sample occurs in a stepwise manner from the outer layer to the core. Since the outermost part (region 1) solidifies first in a short time, by having contact with the cold mold, the volume for the rest is invariant, due to the formation of the outer shell. Though the polymer melt fits well within the volume, it becomes excessive when it solidifies. After most parts (region 1 and 2) become solidified, a considerably larger volume is left for the last part of the polymer melt, which then solidifies as the core with generating a shrinking stress. The solvent is therefore easily absorbed into this region, and has a large motional freedom. We could not carry out a solid-state high-resolution NMR study of this part, since the volume is very small, and it is thus difficult to obtain a sufficient volume for the study.

Although the solvent molecule absorbed in region 1 of the RQ-sample shows a very short T_2(P), that for region 2 of the RQ-sample is considerably longer than that for the same region of the GC-sample (Fig. 4). This fact indicates that the motional freedom of the solvent molecule is not governed only by the cooling speed. As mentioned above, a shrinking stress appears in regions 2 and 3 when the sample is made by rapid quenching from the melt. This may work to grow a larger lamellar and to leave a larger amorphous domain in region 2 of the RQ-sample. This interpretation is in accord with the fact that $T_{1\rho}$ of the crystalline part of this region is longer than those for region 1 of the same sample and region 2 of the GC-sample.

Conclusion

The solvent-probe NMR image of a linear low-density polyethylene rod shaped by rapid quenching of the melt with a metallic mold showed a layered structure. This structure is due to the fact that the spin–spin relaxation time (thus the mobility) of the solvent molecule absorbed in the sample rod is different from one layer to another. This result has been explained in terms of the microstructure in each layer of the matrix polyethylene: i.e. the domain structure of the amorphous and the crystalline region. The solid state characteristics of these different regions of the matrix polyethylene were elucidated from the ^{13}C and ^{1}H relaxation times, which are also different from region to region. It is suggested that in the RQ-sample the outermost region was first solidified and worked to generate stress in the inner region when it solidified. We believe that this kind of utility of NMR imaging technique can be called "solvent-probe NMR imaging".

We thank professor Junkichi Sohma of Kanagawa University for valuable discussion. This work was supported by Grand-in-Aid for Scientific Research on Priority Area "Molecular Magnetism" (Area No. 228/04242102) from the Ministry of Education, Science and Culture.

References

1) R. R. Ernst, G. Bodenhausen, and A. Wokaun, "Principles of Nuclear Magnetic Resonance in One and Two Dimensions," Oxford University Press, Oxford (1987), Chap.

10.

2) D. G. Cory, *Ann. Rep. NMR Spectrosc.*, **24**, 88 (1992).

3) C. Chang and R. A. Komoroski, *Macromolecules*, **22**, 600 (1989).

4) R. S. Clough and J. L. Koenig, *J. Polym. Sci., Polym. Lett. Ed.*, **27**, 451 (1989).

5) L. A. Weisenberger and J. L. Koenig, *Macromolecules*, **23**, 2445, 2454 (1990).

6) L. A. Weisenberger and J. L. Koenig, *J. Polym. Sci., Polym. Lett. Ed.*, **27**, 55 (1989).

7) C. -Y. Hui, K. -C. Wu, R. C. Lasky, and E. J. Kramer, *J. Appl. Phys.*, **61**, 5137 (1987).

8) M. Okazaki and K. Toriyama, *Appl. Magn. Reson.*, **2**, 587 (1991).

9) W. A. Edelstein, J. M. S. Hutchinson, G. Johnson, and T. Redpath, *Phys. Med. Biol.*, **25**, 751 (1980).

10) D. Torchia, *J. Magn. Reson.*, **30**, 613 (1978).

11) M. Iwasaki, F. N. Fritsch, and K. Hedberg, *Acta Crystallogr.*, **17**, 533 (1964).

12) W. L. Earl and D. L. VanderHart, *Macromolecules*, **12**, 762 (1979).

13) D. E. Axelson, L. Mandelkern, R. Popli, and P. Mathieu, *J. Polym. Sci., Polym Phys. Ed.*, **21**, 2319 (1983).